Beta-Catenin and Estrogen Signaling Collaborate to Drive Cyclin D1 Expression in Developing Mouse Prostate

William A. Mulligan[a,b], **Kyle A. Wegner**[c], **Kimberly P. Keil**[b], **Vatsal Mehta**[b], **M. Mark Taketo**[d], and **Chad M. Vezina**[a,b,c,e]

[a]George M. O'Brien Benign Urology Center, University of Wisconsin-Madison, 1656 Linden Drive, Madison, Wisconsin 53706, USA

[b]School of Veterinary Medicine, University of Wisconsin-Madison, 1656 Linden Drive, Madison, Wisconsin 53706, USA

[c]Molecular and Environmental Toxicology Center, University of Wisconsin-Madison, 1656 Linden Drive, Madison, Wisconsin 53706, USA

[d]Division of Experimental Therapeutics, Graduate School of Medicine, Kyoto University Yoshida-Konoé-cho, Sakyo, Kyoto 606-8501, JAPAN

Abstract

Androgen, beta-catenin (CTNNB1), and estrogen pathways stimulate proliferative growth of developing mouse prostate but how these pathways interact is not fully understood. We previously found that androgens induce CTNNB1 signaling in mouse urogenital sinus (UGS) epithelium from which prostatic ductal epithelium derives. Others have shown that low estradiol concentrations induce UGS epithelial proliferative growth. Here, we found that CTNNB1 signaling overlaps cyclin D1 (CCND1) expression in prostatic buds and we used a genetic approach to test whether CTNNB1 signaling induces CCND1 expression. We observed an unexpected sexually dimorphic response to hyperactive CCNTB1 signaling: in male mouse UGS it increased *Ccnd1* mRNA abundance without increasing its protein abundance but in female UGS it increased *Ccnd1* mRNA and protein abundance, suggesting a potential role for estrogens in stabilizing CCND1 protein. Treating wild type male UGS explants with androgen and either 17β-estradiol or a proteasome inhibitor increased CCND1 protein and KI67 labeling in prostatic bud epithelium. Together, our results are consistent with an epithelial proliferative growth mechanism linking CTNNB1-driven *Ccnd1* transcription and estrogen-mediated CCND1 protein stabilization.

Keywords

Prostate development; Ccnd1; estrogen; Ctnnb1; androgen

[e]To whom correspondence should be addressed at chad.vezina@wisc.edu.

1. Introduction

Coordinated cell proliferation guides formation of normal tissue structure in the fetus and maintains tissue homeostasis in the adult. In endocrine-responsive tissues such as the prostate, hormones control cell proliferation across nearly all stages of life. Understanding how hormones interact with each other as well as cell cycle factors is paramount to understanding endocrine organ development and homeostasis.

This study examines the interaction between hormones and proliferative growth signaling pathways in developing mouse prostate. Mammalian prostate derives from the urogenital sinus (UGS) a transient fetal structure positioned between the bladder and urethra. The mouse UGS is an intriguing organ from which to investigate interactions between sex hormones and cell proliferation because both male and female UGS respond to androgens and estrogens. Androgen receptors are detectable in the UGS of both sexes and when activated, drive mouse prostate development in both sexes (Takeda and Chang, 1991; Takeda et al., 1986). Estrogen receptors are also expressed by male and female UGS (Omoto et al., 2005). While neither 17β-estradiol nor estrogen receptor α and β are required for normal prostatic bud formation, their activation can augment androgen-induced prostate proliferative growth (Allgeier et al., 2008; Bianco et al., 2006; McPherson et al., 2001; Prins et al., 2001; Timms et al., 2005; vom Saal et al., 1997; Welshons et al., 2003). Pinpointing downstream targets of androgen and estrogen signaling pathways will help to elucidate how these pathways interact to drive prostate proliferative growth.

To elucidate mechanisms of androgen signaling in developing prostate, we previously compared expression of hundreds of mRNAs across male and female mouse UGS (Abler et al., 2011a; Georgas et al., 2015) and gudmap.org. We found that CTNNB1-responsive transcripts are detected in male but not female UGS epithelium and that functional androgen receptors are required for CTNNB1 target gene expression (Mehta et al., 2011). Subsequent studies offered evidence of a CTNNB1 requirement in specifying UGS epithelium into prostate epithelium and for prostatic bud formation (Francis et al., 2013; Mehta et al., 2013; Simons et al., 2012). Though these studies link androgens to CTNNB1 signaling and prostate development, how CTNNB1 guides proliferative growth processes in the UGS and prostate has yet to be elucidated.

Cyclin D1 (CCND1) interacts with cyclin-dependent kinases and the retinoblastoma protein to promote G1 to S phase progression of the cell cycle (Baldin et al., 1993) and has been identified as a direct transcriptional target of CTNNB1 signaling in multiple organs (Kikuchi, 2000; Lin et al., 2000; Tetsu and McCormick, 1999). CTNNB1 signaling stimulates CCND1 and cellular proliferation in the stomach (Soutto et al., 2015), uterus, breast (Lin et al., 2000; Liu et al., 2014), and colon (Tetsu and McCormick, 1999). Whether CTNNB1 activates CCND1 and proliferative growth in prostatic development has not been examined.

This study's objective was to spatially map CCND1 in the developing mouse prostate and examine its regulation by androgen, estrogen, and CTNNB1 signaling. CCND1 was noticeably more abundant in male compared to female UGS and within males, was

regionally abundant in prostatic bud tips where proliferating cells are concentrated and CTNNB1 signaling is enriched. Yet, while genetic activation of CTNNB1 signaling induced *Ccnd1* mRNA expression in male and female UGS, it only increased CCND1 protein in females. Using UGS explant cultures, we determined that a low (100 pM) concentration of 17β-estradiol combined with androgen increased CCND1 protein expression more than androgen alone. We also found that combining androgen with proteasome inhibition, a known function of estrogen signaling (Zhou et al., 2014), mimicked the actions of estrogen by increasing the number of CCND1 protein-positive prostatic bud epithelial cells. Together, our results are consistent with a mechanism by which androgens activate CTNNB1 signaling in UGS epithelium to stimulate *Ccnd1* transcription and estrogens stabilize CCND1 protein levels to augment proliferative growth. This mechanism may underlie previous observations of estrogen-mediated increases in prostatic growth and development.

2. Materials and Methods

2.1. Animals

C57BL/6J mice (Stock #000664) and *Shh$^{tm2(cre/ERT2)Cjt}$/J* mice (Stock #005623) (Harfe et al., 2004) were purchased from Jackson Laboratory (Bar Harbor, ME). *Ctnnb1$^{tm1Mmt/tm1Mmt}$* mice (Harada et al., 1999) were from Makoto Mark Taketo (Kyoto University, Japan). Mice were housed in polysulfone cages containing corn cob bedding and maintained on a 12 h light and dark cycle at 25 ± 5 °C and 20–50% relative humidity. Feed (Diet 2019 for males and Diet 7002 for pregnant females, Harlan Teklad, Madison, WI, USA) and water were available ad libitum. All procedures were approved by the University of Wisconsin Animal Care and Use Committee and conducted in accordance with the NIH Guide for the Care and Use of Laboratory Animals. To obtain timed-pregnant dams, females were paired overnight with males and the next morning was considered 0 days post coitus (dpc). Mice harboring the dominant stable *Ctnnb1* gain-of-function (iGOF) allele in UGS epithelium (*Shh$^{creERT2/+}$*; *Ctnnb1$^{tm1Mmt/tm1Mmt}$*) and genotypic control mice (*Shh$^{+/+}$*; *Ctnnb1$^{tm1Mmt/tm1Mmt}$*) were generated as described previously (Mehta et al., 2013). Dams were euthanized by CO_2 asphyxiation for embryo collection.

2.2. *In situ* hybridization (ISH)

UGSs were fixed overnight in 4% paraformaldehyde (PFA), dehydrated into methanol and stored at −20°C. On the day of sectioning, UGSs were rehydrated into phosphate buffered saline and cut with a vibrating microtome into 50 μm (sagittal) sections as described previously (Abler et al., 2011a; Abler et al., 2011b; Keil et al., 2012a; Keil et al., 2012b). Protocols for polymerase chain reaction-based riboprobe synthesis and ISH staining are at www.gudmap.org. The staining pattern for each hybridized riboprobe was assessed in at least two UGS sections / mouse fetus and at least three litter-independent fetuses. Replicate male and female tissue sections were processed as a single experimental unit to allow for qualitative comparisons among replicates and between males and females. Riboprobes for *Axin2* and *Wif1* were described previously (Keil et al., 2012b; Mehta et al., 2011). The 551 base pair *Ccnd1* (National Center for Biotechnology Information [NCBI] GeneID: 12443) riboprobe corresponds to positions 2813 to 3363 of the NCBI reference sequence NM_007631.2. The primers used for polymerase chain reaction amplification were 5′-TGG

GAC CAC ATG GGA CAG-3′ and 5′-CGA TGT TAA TAC GAC TCA CTA TAG GGA CCG GAG ACT CAG AGC AAA TC-3′. A synthetic T7 RNA polymerase recognition sequence was incorporated into the reverse primer (underlined).

2.3. Immunohistochemistry (IHC)

Immunofluorescent staining of paraffin sections was performed as described previously (Abler et al., 2011a; Mehta et al., 2011). Antibodies include: rabbit anti-CCND1 (Abcam #ab16663 Cambridge MA), mouse anti-CTNNB1 (BD Transduction labs # 610153, San Jose, CA), rabbit anti-KI67 (Abcam #ab15580), Alexafluor 488-conjugated goat anti-rabbit IgG (Jackson ImmunoResearch #115-547-003, West Grove, PA), Alexafluor 594-conjugated goat anti-mouse IgG (Jackson ImmunoResearch #111-516-045). Tissue sections were also stained with 4′,6-diamidino-2-phenylindole, dilactate (DAPI) to label cell nuclei.

2.4. Organ Culture

14 dpc wild-type male and female UGSs were grown for 4 days on 0.4-µm Millicell-CM filters (Millipore, Billerica, MA) as described previously (Vezina et al., 2008). Media were supplemented with 5α-dihydrotestosterone (DHT; 10 nM, Sigma, St. Louis MO), 17-β estradiol (10 nM or 100 pM, Sigma Aldrich), and the proteasome inhibitor Z-Leu-Leu-Leu-al (10 µM, Sigma). Media and supplements were changed every 2 d.

2.5. Statistical analyses

The percentage of CCND1 and KI67 positive epithelial cells was determined and averaged across 3–5 representative 200X magnified fields from at least 3 mice per group. CTNNB1^{iGOF} cell islands were identified by the presence of detectable cytosolic and nuclear CTNNB1 staining. Statistical analysis was conducted using R version 2.13.1. Student's t-test and analysis of variance (ANOVA) were conducted on untransformed data that passed Bartlett's test for homogeneity of variance and appeared to be normally distributed. Tukey's Honest Significant Difference (HSD) test was used for post-hoc analysis, and p values of less than 0.05 were considered significant. All results are reported as mean ± SE, n ≥ 3 litter independent mice per group.

3. Results and Discussion

3.1. CTNNB1-responsive mRNA expression in prostatic bud tips overlaps CCND1 and KI67 protein expression

Our first objective was to visualize and spatially map CCND1 protein distribution in 18 dpc wild type male and female mouse UGS. In male UGS, CCND1 immunolabled cells were concentrated in prostatic bud tips and were rare in non-budding epithelium and mesenchyme (Fig 1A–B). By contrast, CCND1 immunolabeled cells were rare across the entire female UGS (Fig. 1A–B), indicating androgens potentially support CCND1 expression in male UGSs. CCND1 drives the G1 to S cell cycle transition and we observed many CCND1 and KI67 co–labeled male UGS epithelial cells (Fig 1C). CTNNB1 stimulates *Ccnd1* transcription in the mammary gland (Yan et al., 2011) and colon (Tetsu and McCormick, 1999). *In situ* hybridization revealed the domain of CTNNB1-responsive *Axin2* and *Wif1* mRNAs overlaps the domain of *Ccnd1* mRNA in prostatic bud tips of wild type male UGSs

(Fig 1D–F). Together these results support an enrichment of CCND1 protein in wild type male compared to female UGS and spatially co-localize CCND1 protein expression to a region of active CTNNB1 signaling and active cell proliferation in male mouse prostatic bud epithelium.

3.2. CTNNB1 overexpression is sufficient to increase CCND1 immunostaining in female but not male UGS

We next tested whether hyper-stimulation of CTNNB1 signaling is sufficient to drive CCND1 expression in the UGS. Mice carrying $Shh^{creERT2}$, a tamoxifen-inducible *cre* gene expressed throughout UGS epithelium (Mehta et al., 2013) were bred to mice carrying an inducible dominant stable *Ctnnb1* gain of function (iGOF) allele (*Ctnnb1^{iGOF}* mice) (Harada et al., 1999). When subjected to *cre*-mediated recombination, the resulting fetuses express a patchy (mosaic) pattern of functional and highly stable CTNNB1 protein in some UGS epithelial cells and normal CTNNB1 protein expression in other UGS epithelial cells (Mehta et al., 2013). *cre* activity was induced in fetuses by giving tamoxifen to dams on 13 and 14 dpc. Consistent with our previously reported results, 18 dpc *Ctnnb1^{iGOF}* UGSs harbored cell islands featuring excessive CTNNB1 protein in cell membranes, cytoplasm, and nuclei and over-abundant CTNNB1-responsive mRNAs (Mehta et al., 2013). We expected CCND1 protein-positive cells would also be more abundant in CNNTB1 overexpressing cell islands compared to adjacent normal UGS epithelium but found no such enrichment. Surprisingly, female *Ctnnb1^{iGOF}* mouse UGSs differed from males: the percentage of CCND1 immunopositive cells was enriched in CTNNB1 overexpressing cell islands compared to adjacent normal epithelium (Fig 2A–B). Importantly, we did not observe sex differences in the *Ccnd1* mRNA expression pattern in *Ctnnb1^{iGOF}* UGSs (Fig 2C–D). Our results are consistent with the existence of a post-transcriptional enhancer of CTNNB1-driven *Ccnd1* expression in female mouse UGS.

3.3. Low Concentrations of 17β-Estradiol Drive CCND1 Protein Expression in UGS Explants

Since we observed female specific stabilization of CCND1 in CTNNB1 overexpressing epithelium, we next examined the impact of male and female hormones on CCND1 protein expression in the mouse UGS. Wild type male mouse UGSs were isolated prior to prostatic formation (14 dpc) and grown for four days in medium containing either androgen alone (DHT, 10 nM) or in combination with 17β-estradiol (0.1 or 10 nM). Two concentrations of 17β-estradiol were used because high concentrations of estrogens inhibit prostatic budding and low concentrations stimulate it (Timms et al., 2005; vom Saal et al., 1997). UGS explant sections were immunostained to visualize CCND1 positive cells in prostatic bud tips and no significant difference between DHT alone (control) and DHT + 10 nM 17β-estradiol treatment groups was observed (Fig. 3A–B). However, we found that a 0.1 nM 17β-estradiol significantly increased CCND1 immunolabeled prostatic bud epithelial cells (Fig. 3A–B). We conducted dual-labeling studies with KI67 and CCND1 antibodies. 85±3% of CCND1 positive cells were dual-labeled with KI67 (results not shown) and the dual labeling index was not significantly different among treatment groups (results not shown). These results support CCND1 as a proliferative marker in UGS epithelium and indicate that low but not

high concentrations of 17β-estradiol in combination with androgen have the capacity to increase CCND1 protein expression in the male UGS.

3.4. Proteasome inhibition increases CCND1 expression and cell proliferation in prostatic buds

Estrogens can drive cell proliferation by inhibiting ubiquitin/proteasome activity (Zhou et al., 2014) and CCND1 protein can be degraded by a proteasome-dependent mechanism (Diehl et al., 1998). Because 17β-estradiol in combination with androgen increases CCND1 protein expression and because *Ccnd1* mRNA abundance is similar in male and female *Ctnnb1*[iGOF] UGSs but females have higher CCND1 protein levels, we hypothesized that estrogens stabilize CCND1 protein by inhibiting its degradation. To test whether proteasome inhibition enhances CCND1 expression in wild type UGS epithelium, 14 dpc male UGSs were grown for four days in serum-free media containing androgen (DHT, 10 nM) and the proteosome inhibitor Z-Leu-Leu-Leu-al (10 μM) was added 6 hours before the end of the culture period. The proteasome inhibitor increased both the percentage of CCND1-positive UGS epithelial cells and percentage of KI67 positive UGS epithelial cells (Fig 4A–D). Dual labeling studies indicated that 85±3% of CCND1 positive cells were dual-labeled with KI67 and the dual labeling index did not differ among treatment groups (results not shown). This result raises the possibility that estrogen-driven proteasome inhibition contributes to increased CCND1 protein stability in mouse UGS cells primed with enhanced CTNNB1 signaling, though it is also possible that the proteasome inhibitor used in this study acted by a separate and non-overlapping mechanism.

3.5. Conclusions

We propose the following proliferative growth mechanism integrating androgen, CTNNB1, and estrogen signaling in the UGS: testicular androgens drive CTNNB1 signaling in UGS epithelium, stimulating *Ccnd1* transcription. Low levels of 17β-estradiol interact with CTNNB1 signaling to stabilize CCND1 protein and drive cell proliferation. Consistent with this proposed mechanism, we previously found that androgens and androgen receptors are required for CTNNB1-responsive *Axin2* and *Lef1* mRNA expression in UGS epithelium (Mehta et al., 2011). In the current study, we found that CTNNB1-responsive *Axin2* and *Wif1* mRNA expression overlap CCND1 mRNA and protein expression in prostatic bud tips and that low levels of estrogen and a proteasome inhibitor increase CCND1 protein expression in the presence of androgens.

Many previous studies have demonstrate a capacity of estrogen to stimulate proliferative growth of developing mouse prostate as well as prostate cancer. Our results provide a plausible mechanism linking 17β-estradiol to prostate epithelial proliferative growth. 17β-estradiol concentrations are elevated in the amniotic fluid of female mouse fetuses compared to their male littermates (vom Saal, 1989), and it has been argued that estrogen exposure of a male mouse fetus is influenced by intrauterine position. In support of this argument, male fetuses positioned between two female fetuses grow more prostatic buds than males positioned between one female and one male fetus (Timms et al., 1999). Further, low dose exposures to exogenous estrogens can stimulate proliferative growth in the developing prostate (Timms et al., 2005; vom Saal et al., 1997). Our results provide a testable

mechanism by which fetal estrogen exposures interact with androgens to drive proliferative growth in the developing mouse prostate.

Acknowledgments

Abbreviations

CCND1   cyclin D1

CTNNB1   beta-catenin

UGS   urogenital sinus

References

Abler LL, Keil KP, Mehta V, Joshi PS, Schmitz CT, Vezina CM. A high-resolution molecular atlas of the fetal mouse lower urogenital tract. Dev Dyn. 2011a; 240:2364–2377. [PubMed: 21905163]

Abler LL, Mehta V, Keil KP, Joshi PS, Flucus CL, Hardin HA, Schmitz CT, Vezina CM. A high throughput in situ hybridization method to characterize mRNA expression patterns in the fetal mouse lower urogenital tract. J Vis Exp. 2011b; 54:e2912.

Allgeier SH, Lin TM, Vezina CM, Moore RW, Fritz WA, Chiu SY, Zhang C, Peterson RE. WNT5A selectively inhibits mouse ventral prostate development. Dev Biol. 2008; 324:10–17. [PubMed: 18804104]

Baldin V, Lukas J, Marcote MJ, Pagano M, Draetta G. Cyclin D1 is a nuclear protein required for cell cycle progression in G1. Genes Dev. 1993; 7:812–821. [PubMed: 8491378]

Bianco JJ, McPherson SJ, Wang H, Prins GS, Risbridger GP. Transient neonatal estrogen exposure to estrogen-deficient mice (aromatase knockout) reduces prostate weight and induces inflammation in late life. Am J Pathol. 2006; 168:1869–1878. [PubMed: 16723702]

Diehl JA, Cheng M, Roussel MF, Sherr CJ. Glycogen synthase kinase-3beta regulates cyclin D1 proteolysis and subcellular localization. Genes Dev. 1998; 12:3499–3511. [PubMed: 9832503]

Francis JC, Thomsen MK, Taketo MM, Swain A. beta-Catenin Is Required for Prostate Development and Cooperates with Pten Loss to Drive Invasive Carcinoma. PLoS Genet. 2013; 9:e1003180. [PubMed: 23300485]

Georgas KM, Armstrong J, Keast JR, Larkins CE, McHugh KM, Southard-Smith EM, Cohn MJ, Batourina E, Dan H, Schneider K, Buehler DP, Wiese CB, Brennan J, Davies JA, Harding SD, Baldock RA, Little MH, Vezina CM, Mendelsohn C. An illustrated anatomical ontology of the developing mouse lower urogenital tract. Development. 2015; 142:1893–1908. [PubMed: 25968320]

Harada N, Tamai Y, Ishikawa T, Sauer B, Takaku K, Oshima M, Taketo MM. Intestinal polyposis in mice with a dominant stable mutation of the beta-catenin gene. EMBO J. 1999; 18:5931–5942. [PubMed: 10545105]

Harfe BD, Scherz PJ, Nissim S, Tian H, McMahon AP, Tabin CJ. Evidence for an expansion-based temporal Shh gradient in specifying vertebrate digit identities. Cell. 2004; 118:517–528. [PubMed: 15315763]

Keil KP, Mehta V, Abler LL, Joshi PS, Schmitz CT, CMV. Visualization and quantification of mouse prostate development by in situ hybridization. Differentiation. 2012a; 84:232–239. [PubMed: 22898663]

Keil KP, Mehta V, Branam AM, Abler LL, Buresh-Stiemke RA, Joshi PS, Schmitz CT, Marker PC, Vezina CM. Wnt inhibitory factor 1 (wif1) is regulated by androgens and enhances androgen-dependent prostate development. Endocrinology. 2012b; 153:6091–6103. [PubMed: 23087175]

Kikuchi A. Regulation of beta-catenin signaling in the Wnt pathway. Biochem Biophys Res Commun. 2000; 268:243–248. [PubMed: 10679188]

Lin SY, Xia W, Wang JC, Kwong KY, Spohn B, Wen Y, Pestell RG, Hung MC. Beta-catenin, a novel prognostic marker for breast cancer: its roles in cyclin D1 expression and cancer progression. Proc Natl Acad Sci U S A. 2000; 97:4262–4266. [PubMed: 10759547]

Liu Y, Patel L, Mills GB, Lu KH, Sood AK, Ding L, Kucherlapati R, Mardis ER, Levine DA, Shmulevich I, Broaddus RR, Zhang W. Clinical significance of CTNNB1 mutation and Wnt pathway activation in endometrioid endometrial carcinoma. J Natl Cancer Inst. 2014:106.

McPherson SJ, Wang H, Jones ME, Pedersen J, Iismaa TP, Wreford N, Simpson ER, Risbridger GP. Elevated androgens and prolactin in aromatase-deficient mice cause enlargement, but not malignancy, of the prostate gland. Endocrinology. 2001; 142:2458–2467. [PubMed: 11356695]

Mehta V, Abler LL, Keil KP, Schmitz CT, Joshi PS, Vezina CM. Atlas of Wnt and R-spondin gene expression in the developing male mouse lower urogenital tract. Dev Dyn. 2011; 240:2548–2560. [PubMed: 21936019]

Mehta V, Schmitz CT, Keil KP, Joshi PS, Abler LL, Lin TM, Taketo MM, Sun X, Vezina CM. Beta-catenin (CTNNB1) induces Bmp expression in urogenital sinus epithelium and participates in prostatic bud initiation and patterning. Dev Biol. 2013; 376:125–135. [PubMed: 23396188]

Omoto Y, Imamov O, Warner M, Gustafsson JA. Estrogen receptor alpha and imprinting of the neonatal mouse ventral prostate by estrogen. Proc Natl Acad Sci U S A. 2005; 102:1484–1489. [PubMed: 15665095]

Prins GS, Birch L, Couse JF, Choi I, Katzenellenbogen B, Korach KS. Estrogen imprinting of the developing prostate gland is mediated through stromal estrogen receptor alpha: studies with alphaERKO and betaERKO mice. Cancer Res. 2001; 61:6089–6097. [PubMed: 11507058]

Simons BW, Hurley PJ, Huang Z, Ross AE, Miller R, Marchionni L, Berman DM, Schaeffer EM. Wnt signaling though beta-catenin is required for prostate lineage specification. Dev Biol. 2012

Soutto M, Peng D, Katsha A, Chen Z, Piazuelo MB, Washington MK, Belkhiri A, Correa P, El-Rifai W. Activation of beta-catenin signalling by TFF1 loss promotes cell proliferation and gastric tumorigenesis. Gut. 2015; 64:1028–1039. [PubMed: 25107557]

Takeda H, Chang C. Immunohistochemical and in-situ hybridization analysis of androgen receptor expression during the development of the mouse prostate gland. J Endocrinol. 1991; 129:83–89. [PubMed: 2030333]

Takeda H, Lasnitzki I, Mizuno T. Analysis of prostatic bud induction by brief androgen treatment in the fetal rat urogenital sinus. J Endocrinol. 1986; 110:467–470. [PubMed: 3639118]

Tetsu O, McCormick F. Beta-catenin regulates expression of cyclin D1 in colon carcinoma cells. Nature. 1999; 398:422–426. [PubMed: 10201372]

Timms BG, Howdeshell KL, Barton L, Bradley S, Richter CA, vom Saal FS. Estrogenic chemicals in plastic and oral contraceptives disrupt development of the fetal mouse prostate and urethra. Proc Natl Acad Sci U S A. 2005; 102:7014–7019. [PubMed: 15867144]

Timms BG, Petersen SL, vom Saal FS. Prostate gland growth during development is stimulated in both male and female rat fetuses by intrauterine proximity to female fetuses. J Urol. 1999; 161:1694–1701. [PubMed: 10210442]

Vezina CM, Allgeier SH, Fritz WA, Moore RW, Strerath M, Bushman W, Peterson RE. Retinoic acid induces prostatic bud formation. Dev Dyn. 2008; 237:1321–1333. [PubMed: 18393306]

vom Saal FS. Sexual differentiation in litter-bearing mammals: influence of sex of adjacent fetuses in utero. J Anim Sci. 1989; 67:1824–1840. [PubMed: 2670873]

vom Saal FS, Timms BG, Montano MM, Palanza P, Thayer KA, Nagel SC, Dhar MD, Ganjam VK, Parmigiani S, Welshons WV. Prostate enlargement in mice due to fetal exposure to low doses of estradiol or diethylstilbestrol and opposite effects at high doses. Proc Natl Acad Sci U S A. 1997; 94:2056–2061. [PubMed: 9050904]

Welshons WV, Thayer KA, Judy BM, Taylor JA, Curran EM, vom Saal FS. Large effects from small exposures. I Mechanisms for endocrine-disrupting chemicals with estrogenic activity. Environ Health Perspect. 2003; 111:994–1006. [PubMed: 12826473]

Yan L, Della Coletta L, Powell KL, Shen J, Thames H, Aldaz CM, MacLeod MC. Activation of the canonical Wnt/beta-catenin pathway in ATF3-induced mammary tumors. PLoS One. 2011; 6:e16515. [PubMed: 21304988]

Zhou W, Srinivasan S, Nawaz Z, Slingerland JM. ERalpha, SKP2 and E2F-1 form a feed forward loop driving late ERalpha targets and G1 cell cycle progression. Oncogene. 2014; 33:2341–2353. [PubMed: 23770852]

Highlights

- CTNNB1 signaling overlaps CCND1 protein in prostate buds

- 17β-estradiol increases CCND1 protein in mouse UGS epithelium

- A proteasome inhibitor increases CCND1 protein in mouse UGS epithelium
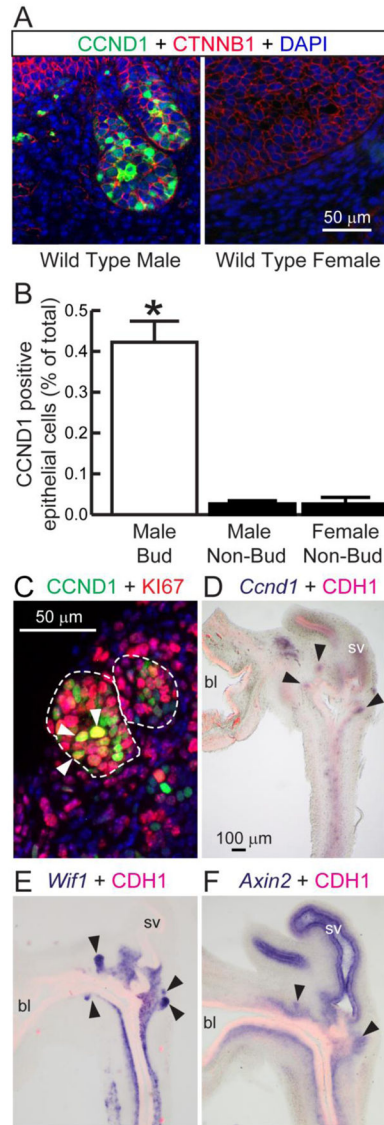
Figure 1. CCND1 protein expression localizes with KI67 and CTNNB1-responsive mRNAs in prostatic bud tips

(A) 18 dpc male and female UGS sections were immunofluorescently stained to detect CCND1 and the UGS epithelial cell marker CTNNB1. Nuclei were stained with DAPI. Staining patterns in each panel represent 3–4 mice. (B) The CCND1 immunolabeling index was determined as the number of CCND1 immunopositive epithelial cells divided by the total number of epithelial cells within a 200X microscopic field. Results are the mean ± SE of three independent samples per group from at least three litters. Asterisks indicate significant differences ($p < 0.05$). (C) 18 dpc male UGS sections were immunofluorescently labeled to detect CCND1 and KI67. Co-labeled cells are indicated by arrowheads. (D-F) 18 dpc male UGS sections were stained by ISH to visualize mRNAs (purple) for *Ccnd1* and the CTNNB1 target genes *Wif1* and *Axin2*. Sections were counterstained by IHC to visualize UGS epithelium marked by e-cadherin (CDH1). Black arrowheads indicate prostatic bud tips. bl: bladder, sv: seminal vesicle.
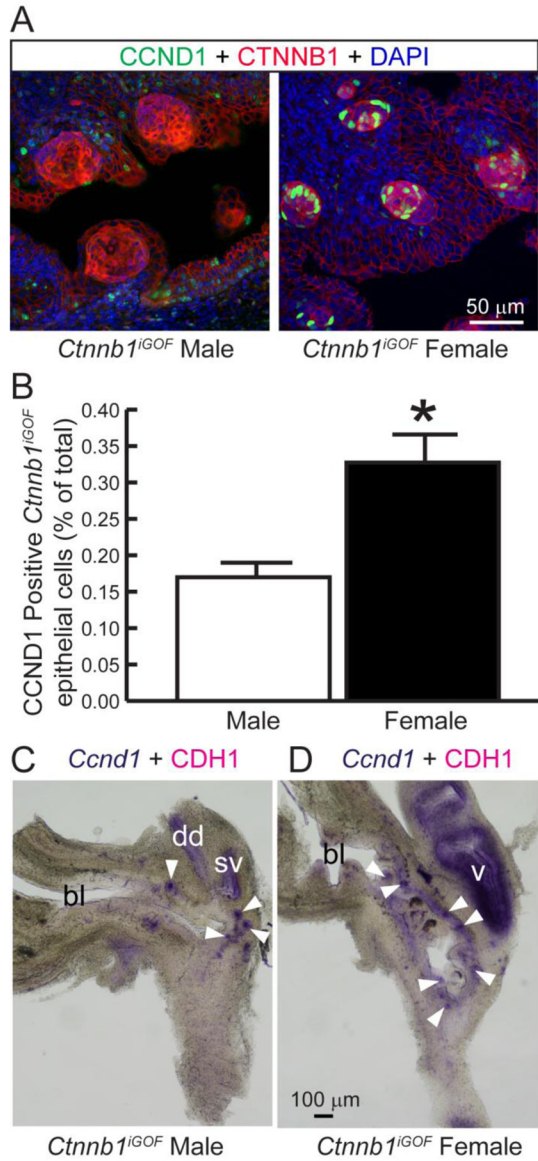
Figure 2. *Ccnd1* mRNA expression is driven by CTNNB1 but CCND1 protein is more abundant in females than males

$Shh^{+/+}$; $Ctnnb1^{tm1Mmt/tm1Mmt}$ (control) and $Shh^{creERT2/+}$; $Ctnnb1^{tm1Mmt/tm1Mmt}$ ($Ctnnb1^{iGOF}$) embryos were exposed to tamoxifen to stabilize CTNNB1 protein in islands of UGS epithelial cells. (A) 18 dpc UGS sections were immunofluorescently labeled to visualize CCND1 and CTNNB1. Staining patterns in each panel represent at least three embryos. (B) The CCND1 immunolabeling index was determined as the number of CCND1 immunopositive epithelial cells divided by the total number of epithelial cells within $Ctnnb1^{iGOF}$ epithelial cell islands. Results are the mean ± SE of three independent samples per group from at least three litters. Asterisks indicate significant differences between groups ($p < 0.05$). (C–D) 18 dpc $Ctnnb1^{iGOF}$ male and female UGSs were stained by ISH to visualize *Ccnd1* mRNA (purple) and counterstained by IHC to visualize UGS epithelium

marked by e-cadherin (CDH1). Arrowheads indicate GOF cell islands. bl: bladder, dd: ductus deferens, sv: seminal vesicle, v: vagina.
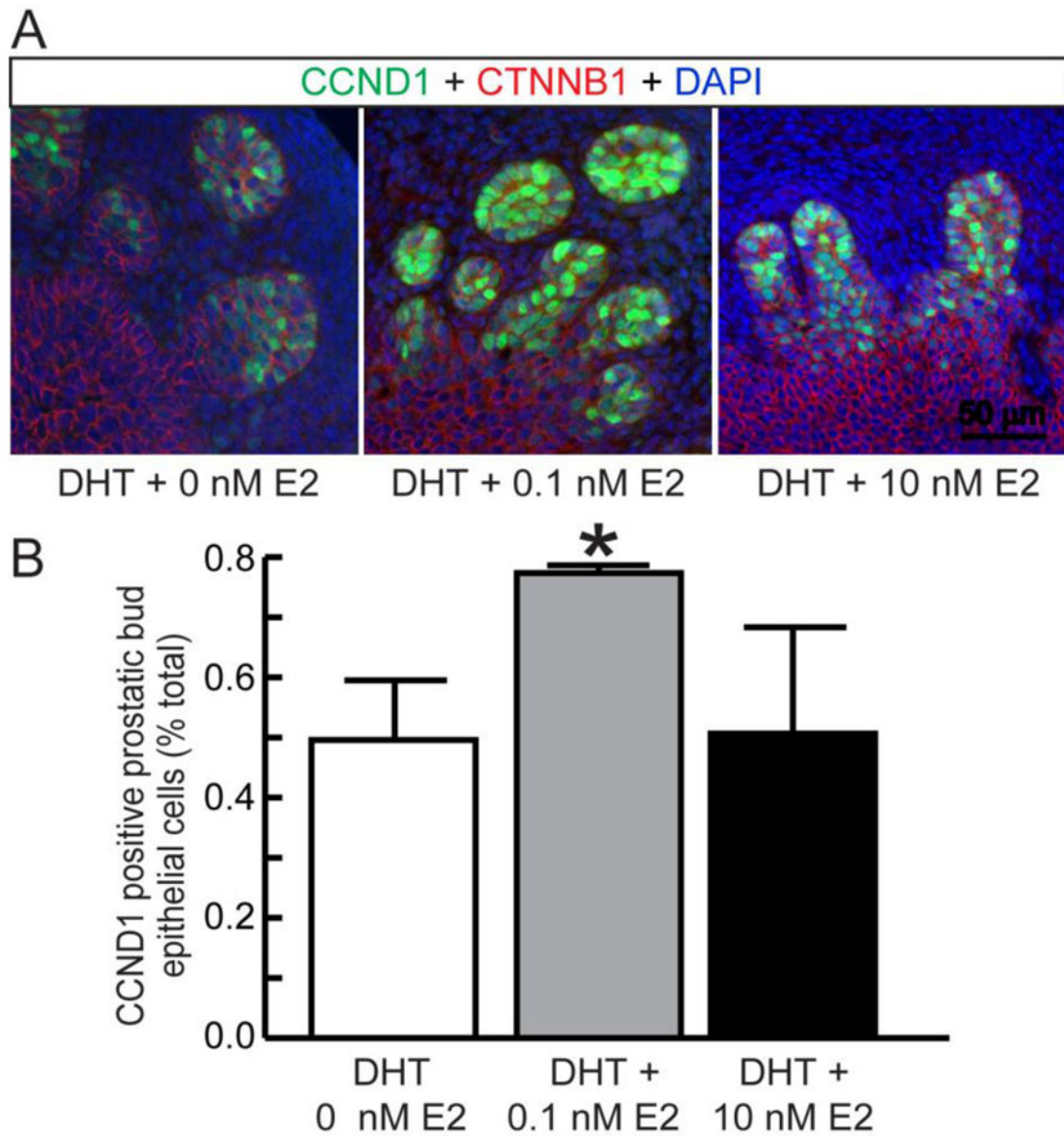
Figure 3. Low estrogen concentrations drive CCND1 expression in mouse UGS explants
14 dpc male mouse UGS explants were grown for 4 days in media containing 5α-dihydrotestosterone (DHT, 10 nM) and vehicle (0.1% ethanol) or DHT and 17β-estradiol (E2, 0.1 nM, 10 nM). (A) 5 μm sections were immunofluorescently labeled to visualize CTNNB1 and CCND1 and cell nuclei were stained with DAPI. (B) The CCND1 immunolabeling index was determined as the number of CCND1 immunopositive prostatic bud epithelial cells divided by the number of visible prostatic bud epithelial bud cells. Results are the mean ± SE of at least three independent samples per group from at least three litters. Asterisks indicate significant differences between groups ($p < 0.05$).
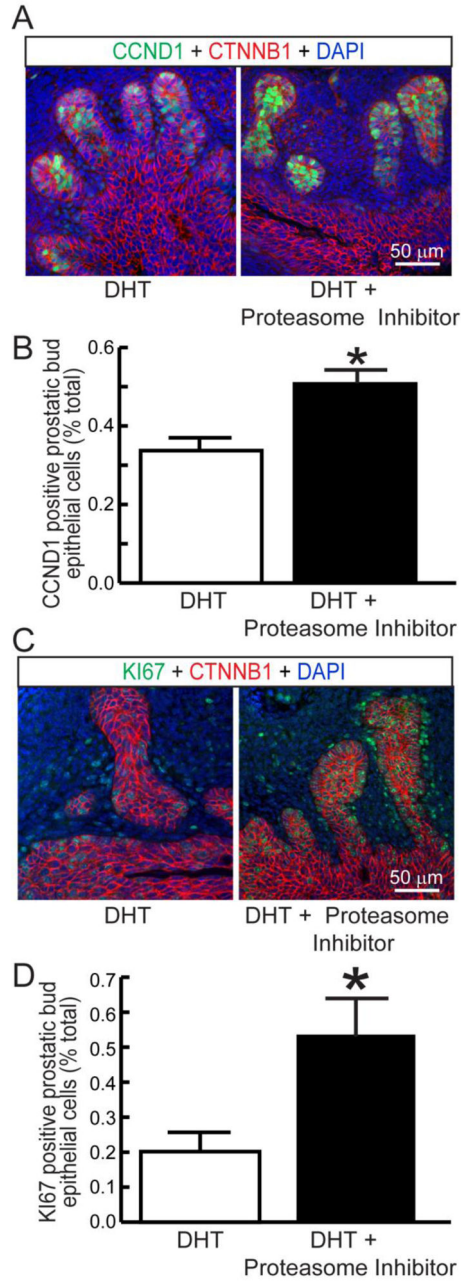
Figure 4. Proteasome inhibition drives CCND1 and KI67 protein expression in mouse UGS explants

14 dpc male mouse UGS explants were grown for 4 days in media containing 5α-dihydrotestosterone (DHT, 10 nM) and vehicle (0.1% DMSO) or DHT and the proteasome inhibitor Z-Leu-Leu-Leu-al (10 mM). 5 μm sections were immunofluorescently labeled to visualize (A) CTNNB1 and CCND1 or (B) CTNNB1 and KI67. Cell nuclei were stained with DAPI. (B, D) CCND1 and KI67 immunolabeling indices were determined as number of prostatic bud epithelial bud cells positive for CCND1 and KI67 divided by the number of

visible prostatic bud epithelial bud cells. Results are the mean ± SE of three independent samples per group from three litters. Asterisks indicate significant differences ($p < 0.05$).